LA-UR- 11-00425

Approved for public release; distribution is unlimited.

Title: Shock compression and spallation of palladium bicrystals with a Σ5 grain boundary

Sigma

Author(s): Sheng-Nian Luo, LANL
Hieu H. Pham, Bedri Arman, Tahir Cagin, Texas A&M University

Intended for: Journal of Applied Physics

Los Alamos
NATIONAL LABORATORY
EST. 1943

Los Alamos National Laboratory, an affirmative action/equal opportunity employer, is operated by the Los Alamos National Security, LLC for the National Nuclear Security Administration of the U.S. Department of Energy under contract DE-AC52-06NA25396. By acceptance of this article, the publisher recognizes that the U.S. Government retains a nonexclusive, royalty-free license to publish or reproduce the published form of this contribution, or to allow others to do so, for U.S. Government purposes. Los Alamos National Laboratory requests that the publisher identify this article as work performed under the auspices of the U.S. Department of Energy. Los Alamos National Laboratory strongly supports academic freedom and a researcher's right to publish; as an institution, however, the Laboratory does not endorse the viewpoint of a publication or guarantee its technical correctness.

Form 836 (7/06)

Submitted to *Journal of Applied Physics*

Shock compression and spallation of palladium bicrystals with a Σ5 grain boundary

Hieu H. Pham,[1] Bedri Arman,[1] S. N. Luo,[2] and Tahir Çağın[1]
[1] *Artie McFerrin Department of Chemical Engineering, Texas A&M University, College Station, Texas 77843, USA*
[2] *Los Alamos National Laboratory, Los Alamos, New Mexico 87545, USA*
(Dated: January 4, 2011)

We investigate an elementary process of shock response of grain boundaries (GBs) using molecular dynamics simulations: shock compression and spallation in Pd bicrystals with a symmetric Σ5/(210)/⟨100⟩ GB. The loading direction is normal to GB. An elastic shock may induce the elastic-plastic or two-wave structure at the GB. The GB serves as a wave scattering center for the transverse motion perpendicular to the GB rotation axis and the shock direction: it induces a phase shift of 180°, an increase in the amplitude of the particle velocity, GB sliding and grain orientation distortion. The GB is the preferred nucleation site both for dislocations and voids. Our results suggest that both microstructure and the loading geometry contribute to dynamic response of a solid.

Shock waves are of interest in a wide range of disciplines and have found a variety of applications.[1,2] While the highly transient nature of shock events makes extremely challenging the real-time measurements of structure responses, molecular dynamics (MD) simulations are useful for understanding at atomistic scales shock physics of a wide range of materials/microstructure, including single crystals, nanocrystalline materials, glasses, polymers, and composites.[3–13] In polycrystalline and nanocrystalline materials, the presence of defects such as grain boundaries (GBs) may have significant effects on "shock response", including dislocation activities, spall damage and wave propagation.[4–6,11,12] It is sometimes beneficial to investigate the interaction of a single GB with shock waves; nonetheless, such studies are scarce and limited to Cu and Al.[9,12,14] Pd, a platinum group metal, is widely used in many applications but the microstructure effect on its shock response is essentially unexplored. Here as a case study, we perform MD shock simulations of a symmetric ⟨100⟩ tilt GB in Pd bicrystals [Σ5/(210)/37°]. The GB leads to wave scattering and sliding at the GB, and serves as the nucleation sites for dislocations and voids.

We use the Large-scale Atomic/Molecular Massively Parallel Simulator (LAMMPS)[15] and an embedded-atom method potential for Pd.[16] Shock wave simulations adopt the flyer-plate–target impact geometry.[17] The impact direction is along [210] (the x-direction) in both the flyer plate and the target, and it is normal to the GB in the latter. The y- and z-axes are along [$\bar{1}$20]) and [001], respectively. The single crystal flyer plate and bicrystal target are constructed separately, and then relaxed and equilibrated at ambient conditions; their dimensions are 525×87×86 Å^3 and 1050×87×86 Å^3, respectively. A bicrystal consists of Crystal 1 and 2 (from left to right), and the GB is located either 525 Å or 700 Å away from the impact plane (corresponding to 1/2 or 2/3 of the bicrystal length). We also construct single crystal target of similar dimensions for comparison. The flyer plate and target are assigned positive and negative velocities along the x-axis, respectively, and then combined (about 800 000 atoms in total). The impact velocity of the flyer plate relative to the target is denoted as $u_{\rm imp}$ (approximately two times the shock-state particle velocity), and is in the range of 0.5–1.3 km s^{-1} in our simulations. Shock simulations are performed with the microcanonical ensemble; periodic boundary conditions are applied only along the y- and z-axes, so there are two free surfaces along the x-axis. The time step for integration of the equation of motion is 1 fs. The local structure is characterized with the centrosymmetry parameter (CS),[18] and local shear, the atomic von Mises shear strain ($\eta_{\rm vM}$).[19] At a given time t, we obtain the profiles of stress (σ_{ij}), velocity (u), density (ρ) and CS via one-dimensional (1D) binning analysis along the shock direction. Similar simulation and analysis details were presented elsewhere.[10,17]

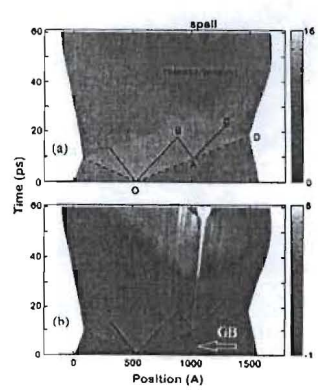

FIG. 1. The x–t diagrams of single crystal–bicrystal impact in terms of ρ (a; in g cm^{-3}) and CS ⟨b). Dashed lines denote elastic wave fronts, and solid lines, plastic shock fronts. The labels are the same in (a) and (b).

The x–t diagrams in Fig. 1 show the sequence of shock compression, release, tension and spallation for the single crystal–bicrystal impact at $u_{\rm imp}$=1.3 km s^{-1} (the GB is in the middle of the bicrystal). Upon collision, shocks propagate into the flyer plate and the target, and are then reflected at the respective free surfaces (e.g., D) as release fans. The superposition of these two release fans induces a tensile region in the target, and leads to spallation if $u_{\rm imp}$ is sufficiently high. Such processes are mani-

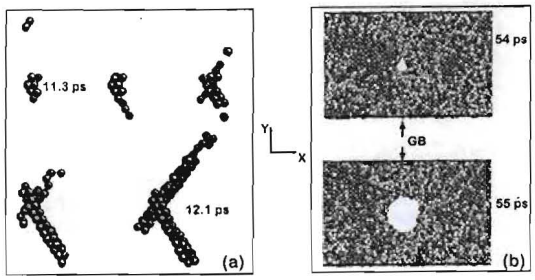

FIG. 4. Snapshots of nucleation and growth of dislocations (stacking faults; a) and a void (b; thin sections) at the GB.

[Fig. 1(b)], as observed previously in Cu.[11,17] The opposing release fans induce an evolving tensile region in the target and tension-induced dislocation activities. The GB "disordering" and plasticity during tension are more pronounced than during compression [Fig. 1(b)].

During tension, the maximum tensile stress ($\sigma_{xx,\max}$) is achieved approximately at the half target thickness, but it does not necessarily represents the spall strength ($\sigma_{\rm sp}$) since spallation depends on microstructure. Fig. 2(d) shows the stress profiles $\sigma_{xx}(x)$ near spallation, which is characterized by stress increase or tensile stress relaxation near the spall plane, the GB. (Spallation is also manifested as density reduction and solid-state disordering; Fig. 1). $\sigma_{\rm sp}$ at the GB is about 20.5 GPa, and $\sigma_{xx,\max}$ is about 20.7 GPa in Crystal 1. $\sigma_{\rm sp}$ for the single crystal under similar loading conditions is about 20−21 GPa. The GB is not considerably weaker likely because the microstructure effect on $\sigma_{\rm sp}$ is less pronounced at extreme strain rates as in our simulations. However, the GB is the preferred void nucleation site. The 1D analysis of ρ and CS shows that spallation plane coincides with the GB (Fig. 1), consistent with direct visualization of the voids during spallation [Fig. 4(b)]. (For the GB located at 2/3 the target length, spallation occurs in Crystal 1 rather than the GB because of insufficient tensile stress at the GB.) Prior to void nucleation, the GB itself undergoes disordering under tension, and tension also induces dislocations emitting from the GB. Similar to compression, tension may also lead to GB sliding and bicrystal distortion. Local heating may be involved as well. These processes as a whole favor the GB for void nucleation. During the void growth, the region immediately surrounding the void is disordered, accompanied by dislocation activities. Such characteristics are also well observed in void nucleation and growth in single crystals and crystals with different defects.[11,17]

Our results show that for the loading geometry explored, the GB serves a wave scattering center for the transverse motion perpendicular to the GB rotation axis and the shock direction: it induces a phase shift of 180°, an increase in the amplitude of the particle velocity, GB sliding and grain orientation distortion. The GB is the preferred nucleation site for dislocations and voids. Both microstructure and the loading geometry contribute to the dynamic response, and their individual contributions and coupling should be incorporated statistically for developing models of complex solids.

This work was supported by ONR as well as LANL's ASC and LDRD programs. Computation was performed at the Texas A&M Supercomputing Facility.

[1] J. R. Asay and M. Shahinpoor, *High-Pressure Shock Compression of Solids* (Springer-Verlag, New York, 1993).

[2] A. Sawaoka, *Shock Waves in Materials Science* (Springer-Verlag, Tokyo; New York, 1993).

[3] T. Germann, B. Holian, P. Lomdahl, and R. Ravelo, Phys. Rev. Lett., **84**, 5351 (2000).

[4] E. Bringa, A. Caro, Y. Wang, M. Victoria, J. McNaney, B. Remington, R. Smith, B. Torralva, and H. Van Swygenhoven, Science, **309**, 1838 (2005).

[5] E. Bringa, A. Caro, M. Victoria, and N. Park, JOM, **57**, 67 (2005).

[6] V. Dremov, A. Petrovtsev, P. Sapozhnikov, M. Smirnova, D. L. Preston, and M. A. Zocher, Phys. Rev. B, **74**, 144110 (2006).

[7] S. G. Srinivasan, M. I. Baskes, and G. J. Wagner, J. Appl. Phys., **101**, 043504 (2007).

[8] V. V. Stegailov and A. V. Yanilkin, J. Exp. Theoret. Phys., **104**, 928 (2007).

[9] C. Pozzi, T. C. Germann, and R. G. Hoagland, in *Shock Compression of Condensed Matter–2009*, Vol. AIP CP1195 (2009) pp. 765–768.

[10] B. Arman, S.-N. Luo, T. C. Germann, and T. Cagin, Phys. Rev. B, **81**, 144201 (2010).

[11] S. N. Luo, T. C. Germann, T. G. Desai, D. L. Tonks, and Q. An, J. Appl. Phys., **107**, 123507 (2010).

[12] S.-N. Luo, T. C. Germann, D. L. Tonks, and Q. An, J. Appl. Phys., **108**, 093526 (2010).

[13] B. Arman, Q. An, S. N. Luo, T. G. Desai, D. L. Tonks, T. Cagin, and W. A. Goddard III, J. Appl. Phys., **109**, xxxxxx (2011).

[14] V. V. Dremov, P. A. Sapozhnikov, and E. M. Bringa, in *Shock Compression of Condensed Matter–2005*, Vol. AIP CP845 (2006) pp. 387–390.

[15] http://lammps.sandia.gov.

[16] X. W. Zhou, J. A. Zimmerman, B. M. Wong, and J. J. Hoyt, J. Mater. Res., **23**, 704 (2008).

[17] S.-N. Luo, Q. An, T. C. Germann, and L.-B. Han, J. Appl. Phys., **106**, 013502 (2009).

[18] C. L. Kelchner, S. J. Plimpton, and J. C. Hamilton, Phys. Rev. B, **58**, 11085 (1998).

[19] J. Li, Modell. Simul. Mater. Sci. Eng., **11**, 173 (2003).

[20] A. Hasnaoui, H. Van Swygenhoven, and P. Derlet, Phys. Rev. B, **66**, 184112 (2002).